

The influence of the global photochemical composition of the troposphere on European summer smog, Part I: Application of a global to mesoscale model chain

Bärbel Langmann

Max-Planck-Institut für Meteorologie, Hamburg, Germany

Susanne E. Bauer

Laboratoire des Sciences du Climat et de l'Environnement, CEA-CNRS, CE SACLAY, L'Orme des Merisiers, Yvette Cedex, France

Isabelle Bey

Swiss Federal Institute of Technology (EPFL), EPFL-ENAC-LMCA, Batiment Chimie, Lausanne, Switzerland

Received 9 January 2002; revised 11 June 2002; accepted 9 December 2002; published 28 February 2003.

[1] Elevated mixing ratios of ozone in the lower troposphere are a major summer time air pollution issue in Europe. Photochemical in-situ production is the most important source of ozone in the planetary boundary layer and has been studied extensively. However, the contributions of background ozone due to stratospheric intrusions, lightning nitrogen oxide followed by ozone production, convective mixing and intercontinental transport are still poorly quantified. We analyze in this paper the influence of the large-scale ozone background on near-surface ozone throughout a summer smog period in July 1994 over Europe. For this purpose a chain of global to mesoscale models is applied with a nesting procedure coupling the individual model simulations. It is found that background ozone as determined by the global model dominates the results of the higher resolution limited area models increasingly with height. But improvements of limited area model results are not only restricted to the free troposphere. Strong convective events like thunderstorms couple free tropospheric and planetary boundary layer air masses so that ozone from above is injected into the planetary boundary layer contributing an amount of 5–10 ppbv to near-surface ozone in the afternoon hours. A decrease in the same range of 5–10 ppbv in maximum near-surface ozone over Central Europe is found in a model simulation where European anthropogenic emissions are reduced by 25%, an amount equal to the reported emission trends in Germany from 1994 to 2000. We conclude that intercontinental transport of pollution can obscure the results of local efforts to reduce critical exposure levels of ozone.

INDEX TERMS: 0345 Atmospheric Composition and Structure: Pollution—urban and regional (0305); 0365 Atmospheric Composition and Structure: Troposphere—composition and chemistry;

0368 Atmospheric Composition and Structure: Troposphere—constituent transport and chemistry;

KEYWORDS: Photochemistry, ozone, 3D-modelling, intercontinental transport

Citation: Langmann, B., S. E. Bauer, and I. Bey, The influence of the global photochemical composition of the troposphere on European summer smog, Part I, Application of a global to mesoscale model chain, *J. Geophys. Res.*, 108(D4), 4146, doi:10.1029/2002JD002072, 2003.

1. Introduction

[2] Enhanced concentrations of photooxidants appear episodically in the planetary boundary layer (PBL) in summertime during high-pressure episodes when direct solar irradiation raises near-surface temperatures. In industrialized regions emissions of photooxidant precursor substances from fossil fuel combustion (NO_x : the sum of NO and NO_2 , and VOCs: volatile organic carbons) and their photo-

chemical transformations are mainly responsible for elevated and episodically critical levels of near-surface ozone and other photooxidants with consequences for human health and plant damages.

[3] When thinking about protection policies, for example, governmental restrictions or guidelines for reduction of industry and traffic emissions during such episodes or on even longer timescales, numerical model simulations help to estimate the potential effects of emission reduction strategies. A huge number of limited area models covering the regions of interest, for example, Europe or North America, have been applied to guide decision makers [Russell and

Dennis, 2000]. The quality of these models is usually tested in hindcast experiments where the calculated distributions of atmospheric trace species are evaluated with available measurements. For such model simulations detailed inventories of emission fluxes are necessary and the meteorological situation of a specific period of interest should be reproduced as realistically as possible. In addition to anthropogenic emissions, biogenic emission fluxes of hydrocarbons have to be specified, although highly uncertain today [Simpson *et al.*, 1999], because these photooxidant precursors often dominate over anthropogenically emitted hydrocarbons, especially during summer smog episodes [Chameides *et al.*, 1988].

[4] Another poorly known topic is the long-range transport of polluted air masses. Stratosphere-troposphere exchange due to irreversible mixing within tropopause folds and/or cut-off lows contribute to the long-range transport and elevated ozone levels in the troposphere [Stohl and Trickl, 1999], sometimes far away from the region of origin. But the overall contribution of stratospheric ozone to the tropospheric ozone budget is still uncertain [Roelofs and Lelieveld, 1997]. The importance of intercontinental transport of photooxidants and precursors in midlatitudes, from Asia to North America [Jaffe *et al.*, 1999, Jacob *et al.*, 1999] and North America to Europe [Li *et al.*, 2001] has been recently emphasised again after first speculations by Parrish *et al.* [1993]. In this context anthropogenic emissions from industry and traffic and biogenic VOC emissions released into the PBL of North America have to be considered, when we focus on Europe, as well as aircraft emissions, NO production by lightning and emissions from forest fires. An impact of Canadian forest fire emissions on Europe throughout the whole summer season is believed to be probable [Forster *et al.*, 2001].

[5] Although it is evident that single continents are not photochemically isolated from the global troposphere, numerical studies with limited area models for Europe or North America have neglected the influence of intercontinental transport of polluted air masses until now. The reason is a lack of detailed information about trace species concentrations throughout the troposphere. Unfortunately, a global observation network including surface based and satellite measurements as it exists for meteorological variables is not yet available for tropospheric trace species. However, within the next few years substantial progress in satellite observations of the tropospheric chemical composition can be expected including vertically resolved information [Singh and Jacob, 2000]. An option that is available today to investigate the large scale distribution of trace species and their temporal and spatial variability in limited area models is a global-regional nesting approach as it is also applied for weather forecast simulations: large scale phenomena are simulated by global coarse grid models and the results are used to provide background concentrations for higher resolution limited area model simulations over the regions of interest.

[6] In this paper, a summer smog episode occurring over Europe at the end of July 1994 is analysed with a global to mesoscale model chain. To our knowledge it is the first time that such a model chain from the global to the mesoscale is used to investigate the question how long-range transport can affect ozone mixing ratios in surface air over Europe

during summer smog episodes. Previous studies of this specific episode have been carried out with prescribed climatological trace species mixing ratios at the lateral model boundaries of a European wide simulation [Bauer and Langmann, 2002b]. These simulations excellently reproduced measured near-surface ozone and nitrogen dioxide mixing ratios at urban stations, whereas in rural areas ozone within the PBL was underestimated. A dramatic underprediction of ozone mixing ratios was also found in the free troposphere. It was suggested that the free troposphere over Europe was significantly influenced by long-range transport of ozone from outside of Europe. Intense convective activity and vertical mixing during this smog episode coupled the PBL and the free troposphere so that the impact of background ozone on near-surface ozone was far from being negligible [Langmann and Bauer, 2002]. In order to arrive at more realistic estimates of the photochemical composition of the troposphere over Europe, we repeated these calculations with time resolved data from a global chemistry transport model [Bey *et al.*, 2001]. The models and their set-ups are introduced in section 2. In section 3 model results are analysed. The individual model strengths and weaknesses are assessed and the powerful application of the combined global to mesoscale model chain is presented. An additional sensitivity simulation is shown which compares the contribution of long-range transported pollution to ozone concentrations at the surface with the effect on ozone levels obtained from local emission reductions. Finally, section 4 draws conclusions and gives an outlook. A detailed analysis of the processes responsible for elevated ozone mixing ratios over Europe in July 1994 is given in a second paper (B. Langmann and I. Bey, manuscript in preparation, 2003).

2. Model Descriptions and Set-Ups

[7] The global to mesoscale model chain used in this study consists of three Eulerian models with a total of four resolutions (Figure 1): The global chemistry-transport model GEOS-CHEM [Bey *et al.*, 2001], the regional atmosphere-chemistry model REMO [Langmann, 2000] applied in two resolutions and the non-hydrostatic mesoscale atmosphere-chemistry model GESIMA [Bauer and Langmann, 2002a]. The simulations with the individual models are carried out one after the other. They are connected by a one-way nesting procedure. Although a nesting factor (ratio of coarse model resolution to nested model resolution) of 3 is referred to as optimal value by Pleim *et al.* [1991] we use nesting factors of 9, 3, and 4.5, respectively. For the global-European nesting step we had no better choice because no other global model simulation was available. For comparison with the global to mesoscale model chain, a mesoscale model chain is run separately (see Figure 1) using fixed climatological trace species distributions for the initialisation and at the lateral boundaries of the European wide simulation. The individual models and set-ups are described only briefly. More detailed information and evaluations can be obtained from the above-cited references.

2.1. The Global Model GEOS-CHEM

[8] The global chemistry-transport model GEOS-CHEM [Bey *et al.*, 2001] is driven by assimilated meteorological

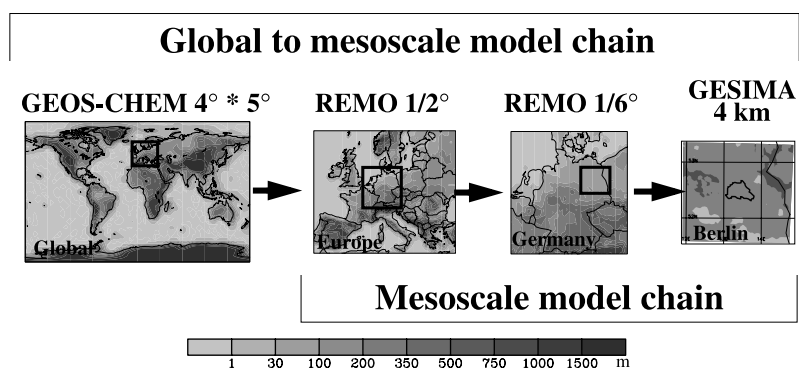


Figure 1. The global to mesoscale model (top) and mesoscale (bottom) chain. Surface orographic is indicated.

observations provided by the Goddard Earth Observing System (GEOS) of the NASA Data Assimilation Office. The data are available every 6 hours on sigma coordinates with 20 vertical levels up to 10 hPa. The horizontal resolution is 2° in latitude and 2.5° in longitude. For computational expediency the GEOS-CHEM simulation is carried out over a $4^\circ \times 5^\circ$ grid with horizontally averaged GEOS data. Advection of 24 chemical trace species is computed every 30 min with a flux-form semi-Lagrangian method as described by *Lin and Rood* [1996]. Moist convection is determined after *Allen et al.* [1996a, 1996b] using the GEOS convective, entrainment and detrainment mass fluxes. Within the atmospheric mixed layer full mixing is assumed diagnosed from surface instability. The tropospheric chemical mechanism of GEOS-CHEM is an updated version of *Horowitz et al.* [1998]. It includes 80 species and 150 reactions with detailed photooxidation schemes for the major hydrocarbons including isoprene. Dry deposition of oxidants and water soluble species is computed using a modified version of *Wesley* [1989]. Anthropogenic emissions are distributed on the basis of inventories for 1985 as described in *Wang et al.* [1998] with updates for 1994 based on energy use statistics as described by *Bey et al.* [2001]. Biomass burning emissions are derived from a climatological inventory [*Wang et al.*, 1998], biogenic emissions are determined with a modified version of the GEIA inventory [*Guenther et al.*, 1995] and NO production by lightning is calculated as described by *Wang et al.* [1998]. A general evaluation of the GEOS-CHEM model has been previously carried out using observations from surface sites, NASA/GTE aircraft campaigns, and ozonesondes [*Bey et al.*, 2001]. No global bias was found for the key species (e.g., ozone, NO, or PAN) except for CO concentrations, which were systematically underestimated by 10 to 20 ppb.

[9] The GEOS-CHEM simulation is conducted from 1 June 1993 to 31 August 1994 starting from climatological trace species distributions as initial conditions. This provides a one-year initialisation until June 1994. Model results from July 1994 are used in this study for comparison with observations and for the nesting of the higher resolution European wide REMO simulation.

2.2. The Regional Model REMO

[10] The regional on-line atmosphere-chemistry model REMO [*Langmann, 2000*] determines at every model time step the physical and chemical state of the model atmos-

phere. The dynamical part and the physical parameterisation routines are taken from the regional weather forecast model system EM/DM of the German Weather Service [*Majewski, 1991*]. In the current study the REMO model is applied with 20 vertical layers of increasing thickness between the Earth surface and the 10 hPa pressure level using terrain following hybrid pressure-sigma coordinates. The horizontal resolution is 0.5° for the model domain covering Europe and $1/6^\circ$ for the smaller area covering Germany (Figure 1). The corresponding model time steps are 5 and 2 min, respectively. The prognostic equations for surface pressure, temperature, specific humidity, cloud water, horizontal wind components and chemical trace species mixing ratios are written on an Arakawa-C-grid [*Mesinger and Arakawa, 1976*]. Tracer transport of 39 species is represented by horizontal and vertical advection according to the algorithm of *Smolarkiewicz* [1983], convective up and downdraft by the mass flux scheme of *Tiedtke* [1989], vertical diffusion after *Mellor and Yamada* [1974] and dry deposition after *Wesley* [1989]. The RADM II chemical scheme [*Stockwell et al.*, 1990] describes photochemical production and loss of 63 compounds by 163 chemical reactions in the gas phase including a wide range of hydrocarbon degradation reactions. Aqueous phase chemistry processes and wet removal are implemented according to *Walcek and Taylor* [1986]. Photolysis rates are calculated as described by *Madronich* [1987] and *Chang et al.* [1987]. Anthropogenic emission data are provided by the Institute of Energy Economics and the Rational Use of Energy, Stuttgart, Germany (B. Wickert, personal communication, 2001) in $1/2^\circ$ resolution for the European model area and consistently in $1/6^\circ$ resolution for the German model area. Biogenic VOC emissions are determined based on *Guenther et al.* [1991, 1993].

[11] To force the two REMO model simulations focussing on Europe and Germany to stay close to the real weather situation, time varying fields of surface pressure, temperature, horizontal wind velocities and moisture derived from the meteorological analysis data of the German Weather Service are used as initial and boundary information, updated every 6 hours. The model is run in the forecast mode with respect to the model physics. Starting at 0 UTC every day a 30-hour forecast is computed. The first six hours are used to spin-up the model physics and are run without chemistry. During the following 24 hours atmospheric physics and chemistry are calculated continuously. At 6 UTC on the following day a discontinuity in the

Table 1. Trace Species Information for the European Wide Simulation

Limited Area Model Species	Global Model Species Information and Adaption
SO ₂	-
SO ₄ ²⁻	-
NO ₂	2/3 NO _x ^a
NO	1/3 NO _x
O ₃	O _x ^b - NO _x
HNO ₃	HNO ₃
H ₂ O ₂	H ₂ O ₂
CH ₃ CHO ^c	CH ₃ CHO
HCHO	HCHO
CH ₃ O ₂ H	3/4 CH ₃ O ₂ H
CH ₃ CH ₂ O ₂ H ^c	1/4 CH ₃ O ₂ H
CH ₃ COO ₂ H	-
HCOOH	-
CH ₃ COOH	-
NH ₃	-
N ₂ O ₅	N ₂ O ₅
NO ₃	-
PAN (peroxyacetyl nitrate)	PAN
C ₃ H ₈ ^c	C ₃ H ₈
C ₅ H ₁₂ ^c	2/3 C ₄ H ₁₀ ^c
C ₈ H ₁₈ ^c	1/3 C ₄ H ₁₀ ^c
C ₂ H ₆	C ₂ H ₆
CO	CO
C ₂ H ₄	-
C ₃ H ₆ ^c	9/10 C ₃ H ₆ ^c
C ₄ H ₈ ^c	1/10 C ₃ H ₆ ^c
CH ₃ C ₆ H ₅	-
CH ₃ C ₆ H ₄ CH ₃	-
CH ₃ CO ₂ O	-
PPN (peroxyacetyl nitrates) ^{c, d}	PPN ^c
HONO	-
HNO ₄	HNO ₄
CH ₃ CH ₂ COCH ₃ ^c	CH ₃ CH ₂ COCH ₃ ^c
(CHO) ₂	-
CHOCOCH ₃	-
R-(CO) ₂ -R (dicarbonyls) ^c	-
R-NO ₃ ^c	R-NO ₃ ^c
HOC ₆ H ₄ CH ₃	-
C ₅ H ₈	C ₅ H ₈

^aNO_x = NO + NO₂ + NO₃ + HNO₂.^bO_x = O₃ + O + NO₂ + 2*NO₃.^cLumped species.^dOther than PAN.

physical state of the model atmosphere is introduced due to the new daily meteorological forecast, whereas tropospheric chemistry is calculated continuously during the period from 20 July, 12 UTC, to 30 July, 12 UTC, 1994.

[12] The temporal and spatial variability of trace species mixing ratios for the initialisation and at the lateral boundaries of the European wide REMO simulation is provided by the output of the global GEOS-CHEM simulation. The chemical mechanisms of the GEOS-CHEM and the REMO model are different, especially with respect to the organic part. Alkane chemistry is of comparable complexity in both models. Alkene chemistry is represented by 4 classes in the REMO model and by only 2 classes in the GEOS-CHEM model; however, the latter has more detailed representation of isoprene chemistry. Three aromatic species (toluene, xylene and cresol) are included in the REMO model, whereas the GEOS-CHEM model neglects aromatic chemistry because of the short species lifetimes. Although we are aware this introduces inconsistencies, we use all available trace species mixing ratio information from the global GEOS-CHEM simulation to initialise the European wide

simulation with REMO. These mixing ratios are distributed among the 39 prognostic species of the regional model as summarized in Table 1. The major longer-lived photooxidant and precursor mixing ratios as for O₃, CO, H₂O₂, PAN, C₂H₆ are provided by GEOS-CHEM. The GEOS-CHEM concentrations are interpolated horizontally and vertically to the REMO 1/2° grid following the temperature interpolation technique of *Majewski* [1985]. For those compounds missing in GEOS-CHEM but necessary for the REMO initialisation and at its lateral boundaries, vertical profiles are derived from available measurements during recent years. The mix-

Table 2. Geographical Station Coordinates

Station	Latitude	Longitude	Altitude above sea level [m]
<i>Spain</i>			
La Cartuja	37°12'N	3°36'W	720
Logrono	42°27'N	2°21'W	370
Roquestas	40°49'N	0°30'W	50
Toledo	39°33'N	4°21'W	917
<i>Alps</i>			
Chaumont	47°03'N	6°59'E	1130
Illmitz	47°46'N	16°46'E	117
Ispra	45°48'N	8°38'E	209
Kovk	46°07'N	15°06'E	600
Krvavec	46°17'N	14°32'E	1740
Payerne	46°48'N	6°57'E	510
Rigi	47°04'N	8°28'E	1030
Sion	46°13'N	7°20'E	480
St.Koloman	47°39'N	13°12'E	851
Taenikon	47°29'N	8°54'E	540
<i>Germany</i>			
Ansberg	49°18'N	10°34'E	481
Bassum	52°51'N	8°43'E	52
Brotjackelriegel	48°49'N	13°13'E	1016
Deuselbach	49°46'N	7°03'E	480
Doberlug-Kirchhain	51°39'N	13°35'E	97
Herleshhausen	51°02'N	10°09'E	380
Hohenwestedt	54°06'N	9°40'E	75
Kyritz	52°56'N	12°25'E	40
Leinefelde	51°24'N	10°19'E	356
Lindenberg	52°16'N	14°25'E	98
Lueckendorf	50°50'N	14°46'E	490
Melpitz	51°33'N	13°56'E	86
Neuglobsow	53°09'N	13°02'E	62
Rottenburg	48°29'N	8°56'E	427
Schauinsland	47°55'N	7°54'E	1205
Schleiz	50°34'N	11°49'E	500
Schmuenecke	50°39'N	10°46'E	937
Schwerin	53°39'N	11°23'E	59
Starnberg	48°01'N	11°21'E	729
Teterow	53°46'N	12°37'E	46
Ueckermunde	53°45'N	14°04'E	1
Waldhof	52°48'N	10°45'E	74
Westerland	54°55'N	8°18'E	12
Zingst	54°26'N	12°44'E	1
<i>Great Britain</i>			
Aston Hill	52°30'N	3°20'W	370
Bottesford	52°56'N	0°49'W	32
Bush	55°52'N	3°12'W	180
Eskdalemuir	55°19'N	3°12'W	243
Glazebury	53°28'N	2°28'W	21
Great Dun Fell	54°41'N	2°27'W	847
Harwell	51°34'N	1°18'W	137
Ladybower	53°23'N	1°45'W	420
Lullington Heath	50°47'N	0°11'E	120
Mace Head	53°10'N	9°30'W	15
Sibton	52°18'N	1°28'E	46
Wharley Croft	54°37'N	2°28'W	206

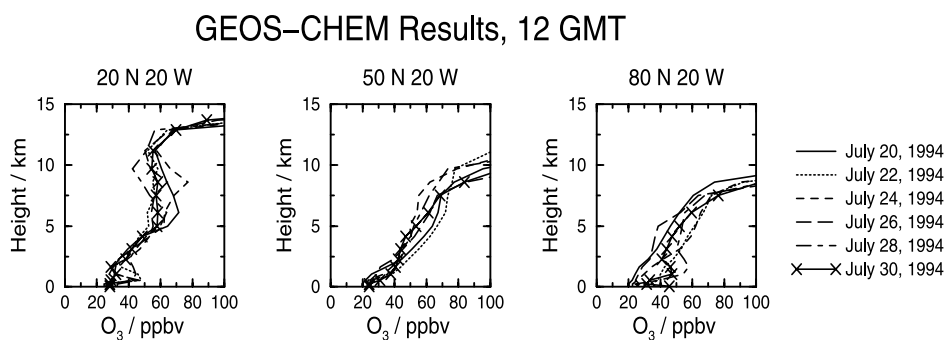


Figure 2. Vertical distribution of 12 UTC ozone in ppbv at [20N, 20W], [50N, 20W] and [80N, 20W] during 20–30 July 1994 as determined by the global GEOS-CHEM model. For clarity reasons the data are shown only in two-day intervals.

ing ratios of the short-lived compounds are set to zero. GEOS-CHEM provides tracer information in 12-hour intervals at 0 and 12 UTC. A linear interpolation in time is carried out to determine the lateral boundary information for the European wide simulation throughout the episode. The 39 chemical trace species mixing ratios are transported by advection across the limited area models lateral boundaries as described by *Pleim et al.* [1991]. Results from this simulation are hereafter denoted as REMO 1/2°.

[13] An additional European wide REMO simulation is carried out with climatological trace species boundary and initial conditions. This set-up corresponds to the usual set-up for limited area air pollution model simulations. Model results from this latter configuration are denoted with an asterisk in the following sections: *REMO 1/2°. For the next nesting step which is the German wide REMO 1/6° simulation nested into the European wide REMO 1/2° simulation the information of the 39 chemical variables is available with a time resolution of one hour. Once again two REMO simulations are carried out: one as part of the global to mesoscale model chain (REMO 1/6°), the other one as part of the mesoscale model chain (*REMO 1/6°).

2.3. The Mesoscale Model GESIMA

[14] The 4 km × 4 km nonhydrostatic meso- γ -scale on-line atmosphere-chemistry model GESIMA [*Bauer and Langmann, 2002a*] is applied over the area of Berlin-Brandenburg, Germany. A detailed description of the dynamical part is given by *Kapitza and Eppel* [1992]. For the numerical solution, the thermodynamic variables are split into isentropic reference values, which are assumed to be hydrostatic, and deviations. For the density, the Boussinesq approximation is used. The model equations are discretised on terrain following coordinates with 25 levels in the vertical up to 11 km height. The basic model time step is 20 seconds. For the horizontal representation orthogonal coordinates with an Arakawa-C-grid are used. Advection of trace species is determined according to *Smolarkiewitz* [1984], vertical diffusion is calculated using a first order closure scheme according to level 2.5 [*Mellor and Yamada, 1974*] and dry deposition is computed after *Wesley* [1989]. Gasphase chemical mechanism, photolysis rates, anthropogenic and biogenic emissions are included in the GESIMA model in the same way as already introduced above for the REMO model.

[15] The GESIMA model uses the following interpolated results of the German wide REMO 1/6° simulation for

initialization: horizontal wind velocities, potential temperature, specific humidity, pressure and trace species mixing ratios. Throughout the simulation (22–26 July 1994) the information of the meteorological variables is nudged at the lateral and top boundaries of the GESIMA model, whereas the information of the chemical species is nested according to *Pleim et al.* [1991]. The data sets are updated every hour with a linear interpolation in between. For more details see *Bauer* [2000].

3. Model Results and Discussion

[16] In this section model results and comparisons with observations are presented and discussed for the period of 20–30 July 1994. We focus on ozone for three reasons: (1) ozone is associated with summer smog, (2) plentiful ozone measurements are available, and (3) ozone is subject to long-range transport in the free troposphere.

3.1. Weather Situation Over Europe

[17] The July 1994 episode was characterised by high surface pressure over Central Europe causing heat waves with maximum near-surface temperatures nearly reaching the highest temperatures ever measured since the beginning of the daily temperature records [*Berliner Wetterkarte, 1994*]. Several low-pressure systems passed over the British Isles and Scandinavia. In the PBL over Central Europe low easterly winds prevailed whereas in the free troposphere westerlies prevailed. Until 25 July dry continental air masses without clouds dominated the weather situation over Central Europe. On 25 July an occlusion with strongly decreasing intensity with time entered Germany from the west, accompanied by moist subtropical air and thunderstorms. During the following days the weather situation remained moist and hot until 29 July, when fresh maritime air was transported toward Germany. Overall, the weather situation favoured photo-smog formation and accumulation in the PBL over Central Europe.

3.2. Large-Scale Distribution of Ozone Outside of Europe

[18] The spatial and temporal variability of ozone mixing ratios as determined by the GEOS-CHEM model at three locations in the Atlantic ocean [20N, 20W], [50N, 20W] and [80N, 20W] is shown in Figure 2 to demonstrate the conditions of the air masses advected toward Europe. The

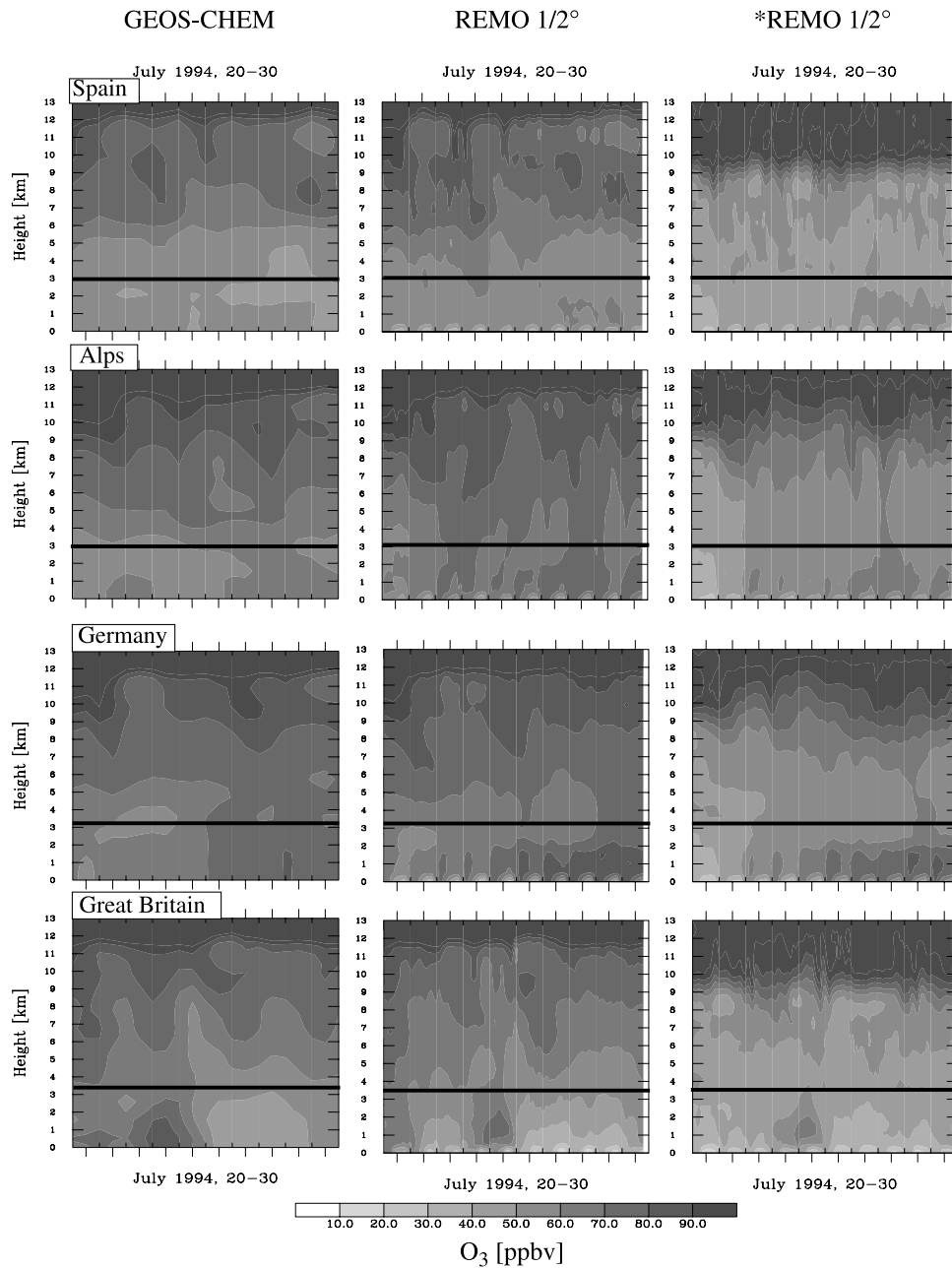


Figure 3. Modelled vertical ozone distribution in ppbv up to approximately 13 km height during 20 July, 12 UTC, to 30 July, 12 UTC, 1994, averaged over 4 European regions following the locations of stations indicated in Table 2: 4 Spanish station (first row), 10 Alpine stations (second row), 24 German stations (third row) and 12 British stations (fourth row). Left column: GEOS-CHEM simulation, mid column: REMO 1/2° simulation, right column: *REMO 1/2°.

increase of ozone mixing ratios above the tropopause clearly indicate the decline of the tropopause altitude with increasing latitude from about 13 km to less than 8 km. Throughout the troposphere a pronounced day-to-day variability of ozone mixing ratios of up to 20 ppbv is visible along the longitude of 20W. PBL mixing ratios at [20N, 20W] and [80N, 20W] were influenced by the nearby landmasses whereas at [50N, 20W] maritime conditions prevail in the PBL. The influence of the temporal and spatial fluctuations of ozone mixing ratios in the downwind direction of Europe on the European photochemical com-

position in the troposphere is further elucidated in the following section.

3.3. Ozone Over Europe

[19] Vertical ozone profiles derived from three model simulations are illustrated in Figure 3 as function of time and averaged over a number of observational stations located in four European subregions: Spain, the Alpine area, Germany, and Great Britain. Table 2 provides the geographical coordinates of the individual stations used in each subregion. Figure 3 shows ozone-mixing ratios from

the GEOS-CHEM simulation and those calculated by the European wide REMO model nested into the GEOS-CHEM simulation (REMO 1/2°). Additionally, results of the European wide REMO simulation with climatological trace species distributions as initial and lateral boundary information denoted *REMO 1/2° are shown in the right hand column of Figure 3. Above about 3 km height the GEOS-CHEM and REMO 1/2° simulation results are very similar with regard to the absolute values of ozone mixing ratios as well as the temporal variability in each of the four European subregions. These similarities were expected since in the free troposphere transport of ozone across Europe occurs faster than photochemical production or loss. Therefore, REMO 1/2° results are closely linked to what is provided as initialisation and at the lateral model boundaries [Langmann and Bauer, 2002], in this case by the GEOS-CHEM simulation. As REMO 1/2° results are presented in 1 hour intervals they show a finer temporal structure compared to the GEOS-CHEM results, which are shown in 12-hour intervals as provided for the nesting procedure. Additional deviations in upper atmospheric ozone can be attributed to differences in the strength and location of convective mixing by the numerous thunderstorms in the two simulations. These differences in the meteorology of the GEOS-CHEM and REMO 1/2° simulations are caused by a factor of nine difference in the horizontal resolutions, the different analysis data sets used to drive the two models and the different model philosophies (CTM/on-line Atmosphere-Chemistry Model).

[20] *REMO 1/2° simulation results for ozone mixing ratios (Figure 3, right-hand column) above 3 km height are completely different from and considerably smaller than the above discussed ozone mixing ratios as determined by GEOS-CHEM and REMO 1/2°. In this case the fixed climatological trace species profiles chosen for the initialisation and at the lateral model boundaries mainly determine *REMO 1/2° results in that altitude region. Hence the importance of reliable assumptions for background mixing ratios is emphasized.

[21] Within the PBL, REMO 1/2° and *REMO 1/2° calculated ozone mixing ratios show a comparable structure in the temporal development throughout the ten days episode, but REMO 1/2° maximum ozone mixing ratios exceed *REMO 1/2° values by about 5–10 ppbv (Figure 3). A pronounced diurnal cycle is visible in both simulations with similar values during the night whereas the GEOS-CHEM simulation does not resolve well this feature because of the too coarse temporal resolution of the boundary related parameters. Modelled and measured near-surface ozone mixing ratios are compared for Spain, the Alpine region, Germany and Great Britain in Figure 4. At the Spanish stations the measured maximum ozone mixing ratios were about 60 ppbv and did not change very much during the episode. The maximum near-surface ozone mixing ratios at the Alpine stations varied around 70 ppbv, at the German stations daily maximum ozone increased from 50 ppbv to 80 ppbv during the episode. GEOS-CHEM calculated values reproduce fairly well the measurements at 12 UTC including the difference of 10 ppbv in maximum ozone between the Spanish and Alpine regions and the ozone increase at the German stations taking into account that maximum near-surface ozone mixing ratios are reached

later in the afternoon. At the British stations daily maximum ozone values are generally overpredicted by up to 25 ppbv by the GEOS-CHEM model.

[22] The best reproduction of maximum ozone mixing ratios shown in Figure 4 is achieved by the global nested REMO 1/2° simulation. This statement is also supported by the scatter diagrams of Figure 5 which show the results of the two European wide REMO simulations for maximum near-surface ozone mixing ratios (hourly data from 12 to 16 UTC) of each station mentioned in Table 2 compared to the observations. Most obvious is the better reproduction of observed maximum ozone mixing ratios in the range of 50–100 ppbv by the global nested REMO 1/2° simulation. The average bias is reduced from –8.1 ppbv for *REMO 1/2° results to –1.6 ppbv for REMO 1/2° results. During the first days the differences in the two REMO results shown in Figure 3 and Figure 4 are mainly caused by the different initial trace species distributions. Afterwards, the two simulations mainly differ because of the imported ozone concentrations into the European area from outside Europe through the lateral boundaries. As the background mixing ratios are the only difference between the two REMO simulations, they are also responsible for the differences in the calculated near-surface ozone mixing ratios. Therefore it can be concluded that during the summer smog episode investigated here, vertical exchange between PBL and free troposphere air masses clearly took place. A significant portion (5–10 ppbv, approximately 5–10%) of near-surface maximum ozone during that episode did not build up from local anthropogenic or biogenic emissions but were due to transport of background ozone from the free troposphere. Our study emphasises the need for using realistic background ozone concentrations throughout the troposphere, which might be different from the climatological values in some cases such as the episode described here, to reduce uncertainties in the simulation of ozone concentrations in the PBL.

[23] The importance of convective events and accompanying rapid subsidence in bringing background ozone from the free troposphere into the PBL is also emphasized by Fiore *et al.* [2002] who studied the origin and contribution of background ozone to photochemical pollution events in the United States during summer. The authors report a contribution of intercontinental transport from Asian and European anthropogenic sources on surface ozone in the United States of 4–7 ppbv in average.

3.4. Photooxidants in the Berlin-Brandenburg Area

[24] For further comparisons of model results and measurements we focus on the area of Berlin-Brandenburg (Figure 1) where a field experiment called FLUMOB (German abbreviation of Aircraft measurements of ozone and precursors to estimate emission reduction measures in Berlin-Brandenburg) took place at the end of July 1994 [Stark *et al.*, 1995]. Aircraft measurements, near-surface measurements and a few vertical soundings were carried out from a ground based observational network. At 27 stations of this network near-surface ozone mixing ratios were measured [see Bauer and Langmann, 2002a, Figure 2]. These data are shown in Figure 6 together with the model results at these stations as determined by the limited area model simulations carried out over the area of Berlin-Brandenburg (*GESIMA

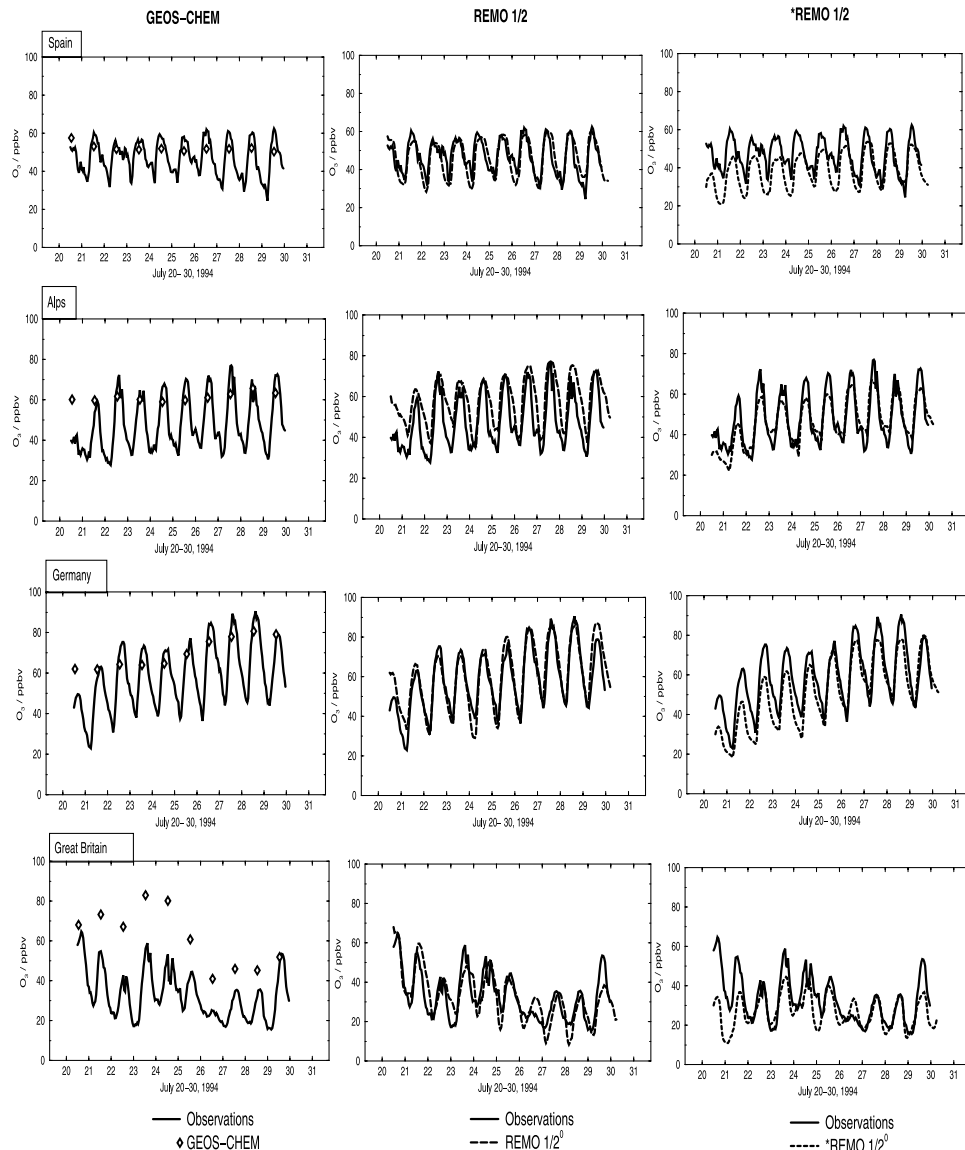


Figure 4. Time series of the measured and modelled (GEOS-CHEM, REMO1/2 and *REMO1/2) near-surface ozone mixing ratios during 20–30 July 1994 averaged over 4 European regions following the locations of stations indicated in Table 2. The GEOS-CHEM simulation does not resolve well the diurnal cycle (see text) so only noon-time values are shown.

and GESIMA), Germany and Europe (Figure 1) in 4 km, $1/6^\circ$ and $1/2^\circ$ horizontal resolution, respectively. The purpose of this comparison is to illustrate the effect of increasing horizontal resolution on the quality of calculated near-surface ozone mixing ratios. With decreasing horizontal resolution the variability of calculated ozone mixing ratios declines. The variability of measured near-surface ozone in the Berlin-Brandenburg area is captured best by the highest resolution simulation with the GESIMA model. The 4 km grid spacing resolves the major highways and industrial sources in that region so that anthropogenic emissions of photooxidant precursor substances can be prescribed in detail (B. Wickert, personal communication, 2001) leading to a more realistic simulation of the variability of secondary pollutants like ozone. Small-scale meteorological phenomena do not influence the GESIMA simulation results significantly during the episode because of the flat topography in the area of Berlin-

Brandenburg and the homogeneous weather conditions. Minimum ozone mixing ratios during the night tend to be underpredicted by GESIMA and slightly overpredicted by the German and European wide REMO simulations whereas the model results for maximum near-surface ozone are rather similar and too low compared to the observations.

[25] Aircraft measurements of ozone and nitrogen dioxide have been carried out in the PBL of Berlin-Brandenburg during the FLUMOB episode at a basic altitude of 500 m with frequent vertical profiling up to about 3 km altitude. The morning and afternoon flights on 25 July 1994 (Figures 7a and 7b) are chosen for comparison with the model simulations. GESIMA results are shown carried out with the whole model chain as indicated in Figure 1 and carried out with the mesoscale part of the model chain only (hereafter: *GESIMA) with climatological trace species distributions at the European model boundaries. Besides ozone

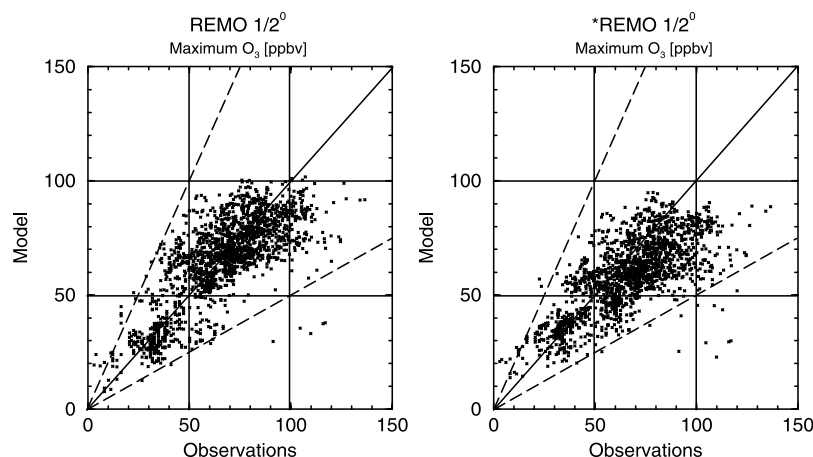


Figure 5. Maximum near-surface ozone mixing ratios (hourly data from 12–16 UTC from all stations mentioned in Table 2) as determined by the global nested REMO $1/2^\circ$ simulation and the *REMO $1/2^\circ$ simulation versus observations for the period 22–30 July 1994. The dashed lines indicate factor of 2 deviations from perfect agreement.

and nitrogen dioxide, Figures 7a and 7b also display the flight tracks and altitudes. The short-lived nitrogen dioxide mixing ratios are reproduced rather well by GESIMA with increasing values in the urban PBL and low values outside the city and above the PBL. The differences in NO_2 mixing ratios between the two GESIMA simulations are negligible, whereas the differences in ozone mixing ratios are significant. Ozone in the PBL as determined by GESIMA is increased by about 5–10 ppbv compared to the *GESIMA simulation and closer to reality. The observed afternoon ozone mixing ratios in the Berlin-Brandenburg area during 22–26 July 1994 range from 50 to 100 ppbv (Figure 6). A threshold value for ozone warning of $180 \mu\text{g}/\text{m}^3$, roughly 90 ppbv in surface air is specified in the EU directives. At least during the few days in July 1994 European anthropogenic and biogenic emission alone would have produced in most cases ozone below the threshold value. A contribution of 5–10 ppbv from background ozone was significant in exceeding the threshold value. During the morning flight (Figure 7a) underprediction of ozone in 500 m altitude is accompanied by elevated NO_2 mixing ratios in both GESIMA simulations. Outside the PBL ozone values are increased up to 20 ppbv in the new GESIMA simulation. The situation in the afternoon hours is different (Figure 7b). Ozone as determined by GESIMA is still underestimated in the PBL and higher up. This points to less vertical mixing, a smaller PBL height, and less photochemical production in the model atmosphere than in reality, or to underestimated free tropospheric background ozone concentrations leading to an underestimation of ozone in the PBL caused by downward mixing. The later explanation is supported by vertical ozone soundings.

[26] Only three ozone soundings were performed during the FLUMOB campaign in the Berlin-Brandenburg area. These measurements starting at Lindenberg (52N, 14E) south east of Berlin are shown in Figure 8 together with simulation results of the REMO model (GESIMA results are not included here because the simulation with that model have been carried out only until 26 July, 0 UTC). The measurements indicate an accumulation of ozone in the

PBL of about 40 ppbv from 23 July to 27 July, the model calculates a smaller increase of about 30 ppbv. The vertical ozone profiles determined by the REMO $1/6^\circ$ simulation are much closer to reality than those of the *REMO $1/6^\circ$ simulation. Again, the two REMO simulation differ by about 5–10 ppbv ozone in the PBL and by up to 20 ppbv ozone in the free troposphere. However, the free troposphere ozone mixing ratios are still significantly too low in the new REMO simulation. Thus, also the free tropospheric input into the PBL is still underestimated in the model.

[27] At this point it should be mentioned that the measured ozone mixing ratios throughout the troposphere at the end of July 1994 were significantly enhanced compared to the climatological mean [Logan, 1999]. A pronounced layering of ozone was observed between 5 and 10 km height on 23 July 1994 (Figure 8) without an associated tropopause-folding event (K. Krueger, personal communication, 2000). Waibel *et al.* [1999] analyzed aircraft measurements of the STREAM II campaign in the tropopause region over the North Sea area during the same period of 20–30 July 1994. Based on backward trajectory analysis the authors concluded that elevated CO mixing ratios in the tropopause region originated from Canadian forest fire emissions. These emissions might also be responsible for the layering of ozone observed over Lindenberg on 23 July 1994. Unfortunately, episodic events of high biomass burning activity are not included in the climatological monthly mean biomass burning emissions inventory of the GEOS-CHEM simulation used in the work shown here. Consequently, a portion of photooxidants formation might be missing in the simulation results presented here. Recently, activities have started to improve the timing of biomass burning emissions during specific periods in global models using satellite observations [Duncan *et al.*, 2003] so that a more realistic representation of these emission can be expected in the future.

3.5. European Emission Reduction Experiment

[28] In this section we show results from a European wide model simulation in which anthropogenic emissions of CO,

Berlin-Brandenburg area

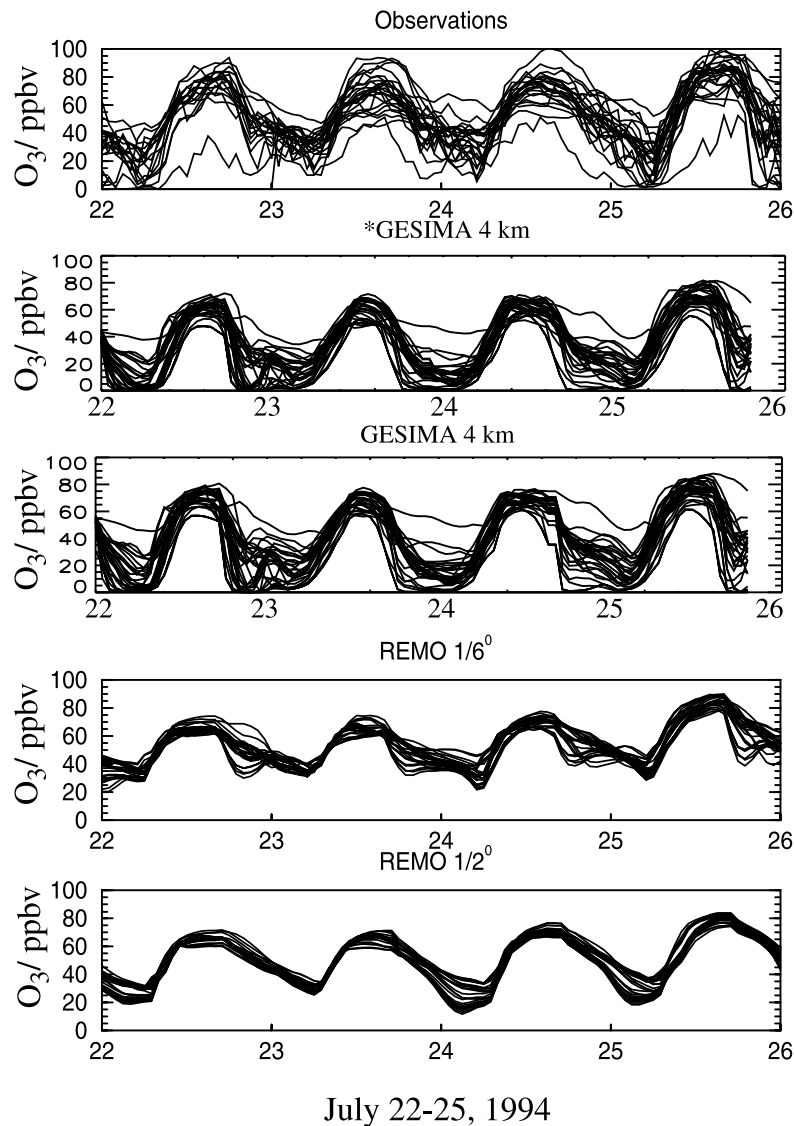


Figure 6. Near-surface ozone mixing ratios at 27 sites in the Berlin-Brandenburg area: Measurements and model results during 22–25 July 1994. For the GESIMA calculations the area of Berlin-Brandenburg is represented by 50×50 grid points. Approximately 11×11 grid points cover the area in the REMO $1/6^\circ$ simulation and only 4×4 grid points in the REMO $1/2^\circ$ simulation.

VOC, NO_x and SO_x are reduced by 25%. This reduction corresponds approximately to the emission decrease of NO_2 in Germany from 1994 to 2000 (Umweltbundesamt data, available from <http://www.umweltbundesamt.de>). The results of the sensitivity experiment, hereafter REMO-red. $1/2^\circ$ are compared to the global nested REMO $1/2^\circ$ simulation presented in section 3.3. The motivation for this sensitivity experiment is to compare the effect of European wide emission reductions with the contribution of long-range transported pollution to ozone concentrations in surface air over Europe during summer smog conditions.

[29] Figure 9 illustrates near-surface ozone mixing ratios determined by the global nested REMO simulation as 4 days average (25–28 July 1994) at 16 UTC and the effect

of the European wide emission reduction experiment. An unexpected small increase of 2.5–5 ppbv ozone is visible over England and the main outflow direction, the North sea area (Figure 9b) which can be explained as follows: Due to the cloudy conditions the absolute ozone values in these air masses are rather small in the range of 20–40 ppbv (Figure 9a). However, the load of pollutants, mainly NO_x is high so that an emission reduction of only 25% leads to a decrease of HNO_3 formation which in turn increases the availability of OH, thus allowing more ozone production [Sillman *et al.*, 1990]. Over Central Europe the emission reduction leads to the expected decrease of the daily ozone maxima. The effect is stronger than 5 ppbv with maximum values of about 10 ppbv. These values are in the same

Flight METAIR July 25, 1994, morning hours

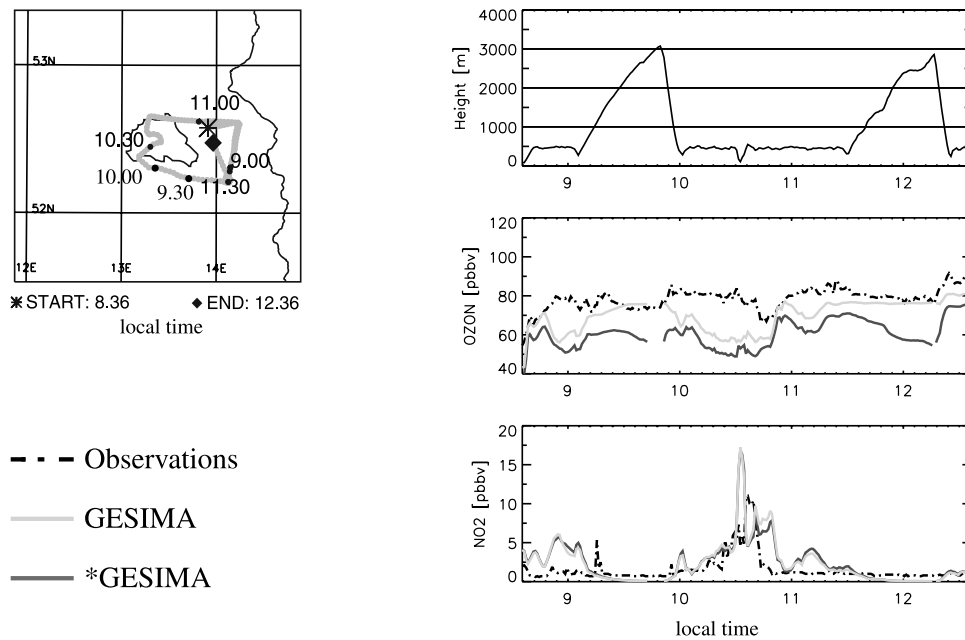


Figure 7a. Aircraft measurements during the morning of 25 July 1994 compared with model results. GESIMA represents global to mesoscale model chain results; *GESIMA represents mesoscale model chain results.

Flight METAIR July 25, 1994, afternoon hours

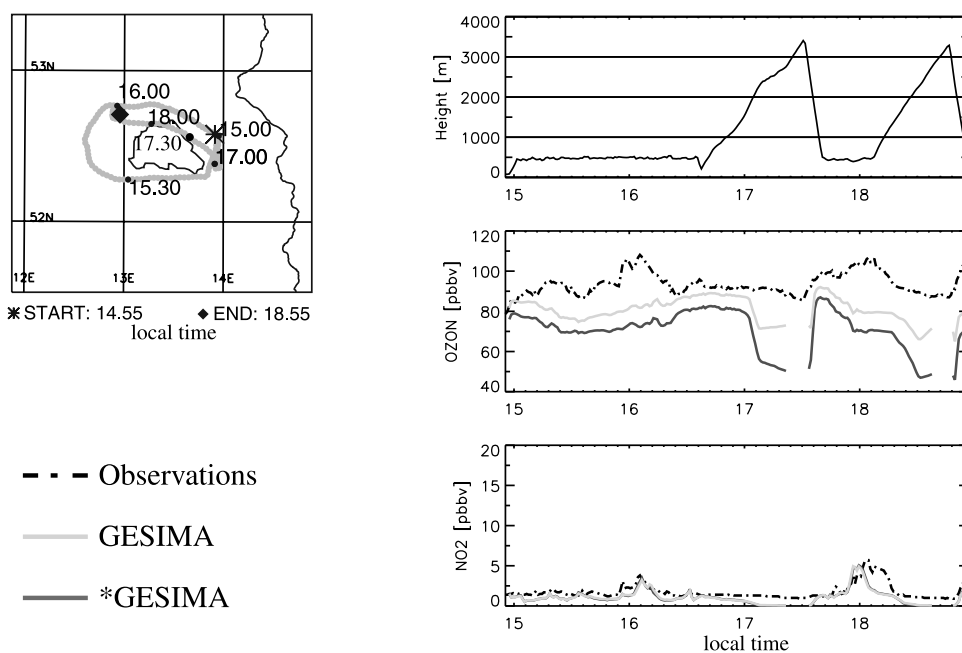


Figure 7b. As in Figure 7a but during the afternoon hours of 25 July 1994.

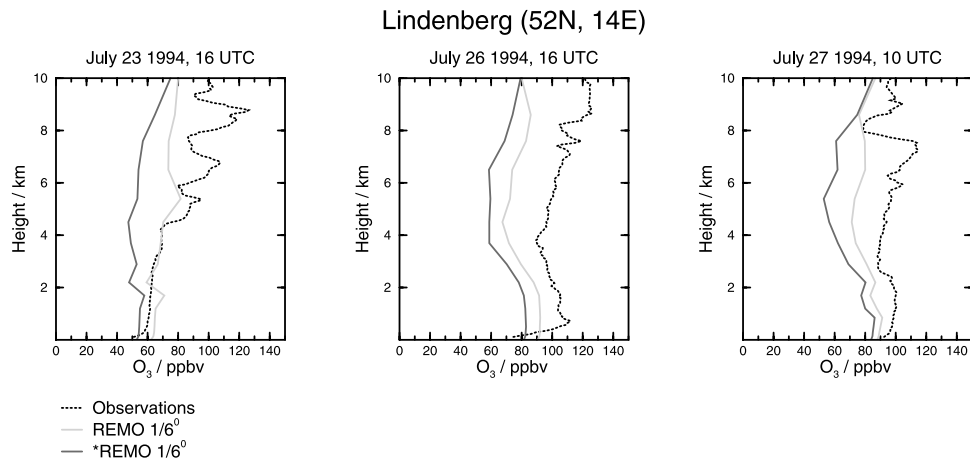


Figure 8. Ozone sonde observations at Lindenberg (52N, 14E) and model results from REMO simulations.

range but opposite direction as those presented in the previous subsections related to the effect of long-range transport of polluted air masses from outside of Europe. Thus, emissions from elsewhere (North America, Asia) and long-range transport increase daily ozone maxima over Europe during summer smog conditions by roughly the same amount as European emission reduction efforts decrease daily ozone maxima.

4. Conclusions and Outlook

[30] A global to mesoscale model chain focussing on Europe, Germany and Berlin-Brandenburg has been applied in this paper for the investigation of the effect of long-range transport of pollution on surface air composition during a summer smog episode at the end of July 1994. Throughout

this period the global model simulation provides a first estimate of the photochemical composition of the troposphere twice the day in a relatively coarse horizontal resolution. Three nesting steps are performed so that the results of the respective lower resolution model simulation are used as initial and lateral boundary data for the respective higher resolution model simulation. Thus, we replaced one unknown contribution in the mathematical formulation of limited area air pollution models, that is, the initial and boundary problem which is usually solved by adjusting boundary conditions within “acceptable” bounds through iterative search for acceptable performance [Russell and Dennis, 2000], by data sets produced by a global model based on physical and chemical principles. The standard practice improves model performance without knowing the reasons, whereas our approach also offers the possibility to

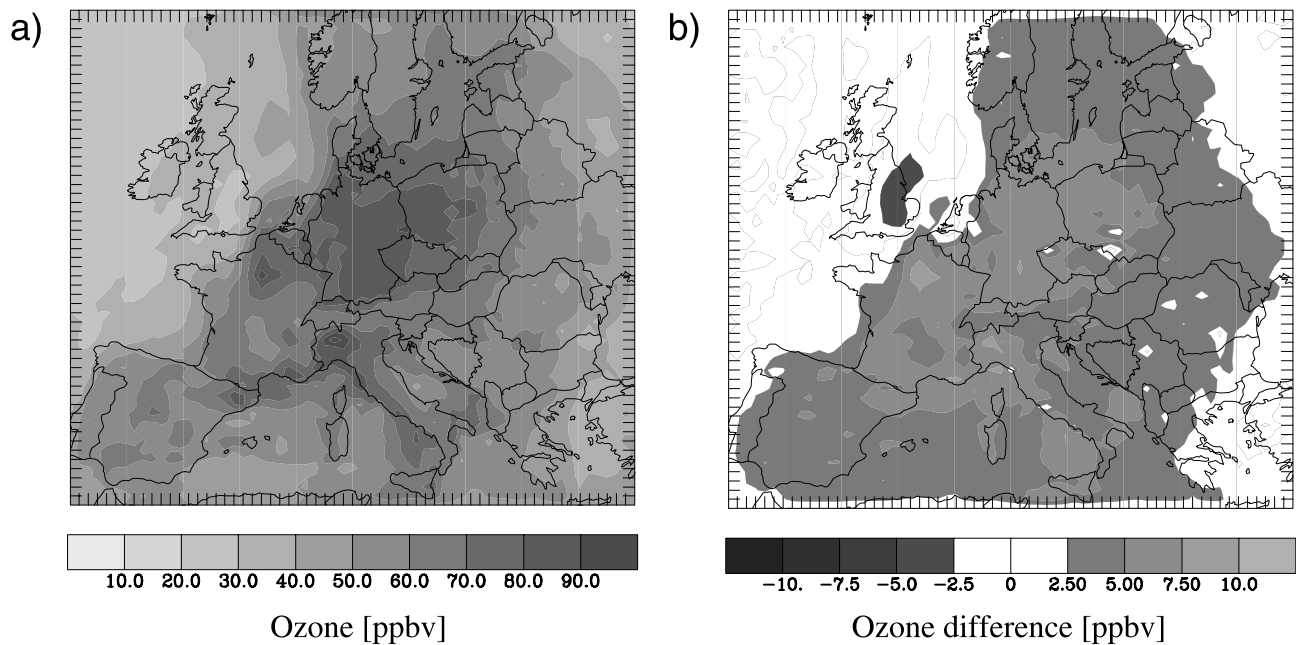


Figure 9. (a) Near-surface ozone mixing ratios as determined by the global nested REMO 1/2° simulation as 4 days average (25–28 July 1994) at 16 UTC together with (b) the difference: REMO 1/2° minus REMO-red. 1/2° simulation results which represent the European wide emission reduction effect.

improve the understanding of the relevant processes that determine tropospheric photochemistry. Nowadays our approach is still expensive and time consuming but will become more appealing in the future with the expected progress in chemical data assimilation and global photochemistry modeling.

[31] The evaluation of model results with near-surface observations of ozone reveals a more realistic reproduction of the variability of simulated ozone mixing ratios with increasing horizontal resolution. Ozone mixing ratios simulated by the mesoscale models in the PBL and the free troposphere are considerably closer to observed levels when initial and lateral boundary conditions are taken from the global model simulation. However, the observed unusually high mixing ratios of ozone in the free troposphere are still underestimated in our model simulations. A detailed analysis of the origin of ozone in the free troposphere over Europe at the end of July 1994 is presented in a companion paper (B. Langmann and I. Bey, manuscript in preparation, 2003) to illuminate the uncertainties and the complex interactions between long-range transport of pollutions, for example, Canadian forest fire emissions as assumed by *Waibel et al.* [1999], local sources, for example, lightning NO_x production and convective mixing.

[32] Ozone mixing ratios determined by the global model dominate the results of the higher resolution limited area models in the free troposphere but also contribute significantly to near-surface ozone mixing ratios. Convective mixing induced by occasionally occurring thunderstorms couple the air masses of the free troposphere and the PBL over Europe. It is shown that ozone from the free troposphere is injected into the PBL contributing an amount of at least 5–10 ppbv to maximum near-surface ozone mixing ratios during the summer smog episode under investigation. It should be noted, however, that the contribution of long-range transported pollution to ozone concentrations in surface air calculated for that period might not be representative of typical situations because of especially high convective activity which contributes significantly to vertical transfer between the PBL and the free troposphere. Further work is needed to evaluate such numbers on a climatological basis.

[33] When reducing anthropogenic emissions by 25% (corresponding approximately to the emission reduction in Germany from 1994 to 2000) in a European wide model simulation we receive again a modification of 5–10 ppbv in maximum near-surface ozone over Central Europe, a decrease in this case. From these results we conclude that intercontinental transport of pollution can obscure the results of local efforts to reduce critical exposure levels of ozone during summer smog conditions. European pollution might also be reduced by decreasing emissions elsewhere due to the decreasing contribution to the long-range transport of pollution. Other aspects that affect the long-range transport of pollution and its impact on European pollution levels are modifications in large-scale dynamics. For example, *Li et al.* [2002] found a high correlation ($r = 0.57$) between the North Atlantic Oscillation (NAO) index and “North American ozone” at Mace Head, a remote site at the Atlantic coast of Ireland for the period 1993–1997. A decline in the NAO index would reduce transatlantic transport of American pollution to Europe. Although in *Osborn*

et al. [1999] a significant decline in the NAO index is predicted using a general circulation model with anthropogenic forcing from greenhouse gases and sulphate aerosols, a new manuscript in preparation by T. J. Osborn [2003] using a pattern-based measure of the NAO concludes the opposite, namely a weak increase in the NAO. This revised result concerning NAO could lead to an increase of transatlantic transport of American pollution to Europe emphasising that global restrictions of anthropogenic CO , VOC and NO_x emissions are necessary to reduce and control the formation of photooxidants.

[34] **Acknowledgments.** The authors would like to acknowledge all the scientists and institutes involved in the development of the numerical models applied in this paper and those who made their data available, and thanks to Christiane Textor and Martin Schultz from the MPI for Meteorology and the two anonymous reviewers for their valuable comments on the manuscript.

References

- Allen, D. J., R. B. Rood, A. M. Thompson, and R. D. Hudson, Three-dimensional radon 222 calculations using assimilated data and a convective mixing algorithm, *J. Geophys. Res.*, **101**, 6871–6881, 1996a.
- Allen, D. J., P. Kasibhatla, A. M. Thompson, R. B. Rood, B. G. Doddridge, K. E. Pickering, R. D. Hudson, and S. J. Lin, Transport induced interannual variability of carbon monoxide using a chemistry and transport model, *J. Geophys. Res.*, **101**, 28,655–28,670, 1996b.
- Bauer, S. E., Photochemical smog in Berlin-Brandenburg: An investigation with the atmosphere-chemistry model GESIMA, Ph.D. Thesis, Examination Rep. No. 81, Max-Planck-Institute for Meteorology, Hamburg, Germany, 2000.
- Bauer, S. E., and B. Langmann, An atmosphere-chemistry model on the meso- γ scale: Model description and evaluation, *Atmos. Environ.*, **36**, 2187–2199, 2002a.
- Bauer, S. E., and B. Langmann, Analysis of a summer smog episode in the Berlin-Brandenburg region with a nested atmosphere-chemistry model, *Atmos. Chem. Phys.*, **2**, 259–270, 2002b.
- Berliner Wetterkarte, available from the Institute for Meteorology, University of Berlin, Carl-Heinrich-Becker-Weg 6-10, 12165 Berlin, Germany, July 1994.
- Bey, I., D. J. Jacob, R. M. Yantosca, J. A. Logan, B. D. Field, A. M. Fiore, Q. Li, H. Y. Liu, L. J. Mickley, and M. G. Schultz, Global modeling of tropospheric chemistry with assimilated meteorology: Model description and evaluation, *J. Geophys. Res.*, **23**, 073–23,096, 2001.
- Chameides, W. L., R. W. Lindsay, J. Richardson, and C. S. Chiang, The role of biogenic hydrocarbons in urban photochemical smog: Atlanta as a case study, *Science*, **241**, 1473–1475, 1988.
- Chang, J. S., R. A. Brost, S. A. Isaksen, S. Madronich, P. Middleton, W. R. Stockwell, and C. J. Walcek, A three dimensional Eulerian acid deposition model: Physical concepts and formulation, *J. Geophys. Res.*, **92**, 14,681–14,700, 1987.
- Duncan, B. N., R. V. Martin, A. C. Staudt, R. Yevich, and J. A. Logan, Interannual and seasonal variability of biomass burning emissions constrained by satellite observations, *J. Geophys. Res.*, **108**, 4100, doi:10.1029/2002JD002378, 2003.
- Fiore, A. M., D. J. Jacob, I. Bey, R. M. Yantosca, and B. D. Field, Background ozone over the United States in summer: origin and contribution to pollution episodes, *J. Geophys. Res.*, **107**, 4275, doi:10.1029/2001JD000982, 2002.
- Forster, C., P. James, G. Wotowa, U. Wandinger, I. Mattis, D. Alshausen, P. Simmonds, S. O’Doherty, S. G. Jennings, C. Kleefeld, J. Schneider, T. Trickl, S. Kreipl, H. Jaeger, and A. Stohl, Transport of boreal forest fire emissions from Canada to Europe, *J. Geophys. Res.*, **106**, 22,887–22,906, 2001.
- Guenther, A. B., R. K. Monson, and R. Fall, Isoprene and monoterpene emission rate variability: Observations with eucalyptus and emission rate algorithm development, *J. Geophys. Res.*, **96**, 10,799–10,808, 1991.
- Guenther, A. B., P. R. Zimmermann, P. C. Harley, R. K. Monson, and R. Fall, Isoprene and monoterpene emission rate variability: Model evaluation and sensitivity analysis, *J. Geophys. Res.*, **98**, 12,609–12,617, 1993.
- Guenther, A., et al., A global model of natural volatile organic compound emissions, *J. Geophys. Res.*, **100**, 8873–8892, 1995.
- Horowitz, L. W., J. Liang, G. M. Gardner, and D. J. Jacob, Export of reactive nitrogen from North America during summertime: Sensitivity to hydrocarbon chemistry, *J. Geophys. Res.*, **103**, 13,451–13,476, 1998.

- Jacob, D. J., J. A. Logan, and P. P. Murti, Effect of rising Asian emissions on surface ozone in the United States, *Geophys. Res. Lett.*, *26*, 2175–2178, 1999.
- Jaffe, D., et al., Transport of Asian air pollution to North America, *Geophys. Res. Lett.*, *26*, 711–714, 1999.
- Kapitzka, H., and D. Eppel, The nonhydrostatic mesoscale model GESIMA, I, Dynamical equations and tests, *Contr. Atmos. Phys.*, *65*, 129–146, 1992.
- Langmann, B., Numerical modelling of regional scale transport and photochemistry directly together with meteorological processes, *Atmos. Environ.*, *34*, 3585–3598, 2000.
- Langmann, B., and S. E. Bauer, On the importance of reliable background concentrations of ozone for regional scale photochemical modelling, *J. Atmos. Chem.*, *42*, 71–90, 2002.
- Li, Q., D. J. Jacob, I. Bey, R. M. Yantosca, B. D. Field, J. A. Logan, A. M. Fiore, R. V. Martin, and B. N. Duncan, Sources of ozone over the North Atlantic and trans-Atlantic transport of pollution: A global model perspective, *IGAC Newsletter*, *24*, 12–17, 2001.
- Li, Q., et al., Transatlantic transport of pollution and its effects on surface ozone in Europe and North America, *J. Geophys. Res.*, *107*, 4166, doi:10.1029/2001JD001422, 2002.
- Lin, S.-J., and R. B. Rood, Multidimensional flux form semi-Lagrangian transport schemes, *Mon. Weather Rev.*, *124*, 2046–2070, 1996.
- Logan, J. A., An analysis of ozonesonde data for the troposphere: Recommendations for testing 3-D models and development of a gridded climatology for tropospheric ozone, *J. Geophys. Res.*, *104*, 16,115–16,149, 1999.
- Madronich, S., Photodissociation in the atmosphere, I, Actinic flux and the effect of ground reflections and clouds, *J. Geophys. Res.*, *92*, 9740–9752, 1987.
- Majewski, D., Balanced initial and boundary values for a limited area model, *Contr. Atmos. Phys.*, *58*, 147–159, 1985.
- Majewski, D., The Europa Modell of the Deutscher Wetterdienst, Seminar proceedings ECMWF, *2*, pp. 147–191, 1991.
- Mellor, B., and T. Yamada, A hierarchy of turbulence closure models for planetary boundary layers, *J. Atmos. Sci.*, *31*, 1791–1806, 1974.
- Mesinger, F., and A. Arakawa, Numerical methods used in atmospheric models, *GARP Publications Series*, No. 17, pp. 1–64, WMO, Geneva, Switzerland, 1976.
- Osborn, T. J., K. R. Briffa, S. F. B. Tett, P. D. Jones, and R. M. Trigo, Evaluation of the North Atlantic Oscillation as simulated by a coupled climate model, *Clim. Dyn.*, *15*, 685–702, 1999.
- Parrish, D. D., J. S. Holloway, M. Trainer, P. C. Murphy, G. L. Forbes, and F. C. Fehsenfeld, Export of North American Ozone Pollution to the North Atlantic Ocean, *Science*, *259*, 1436–1438, 1993.
- Pleim, J. E., J. S. Chang, and K. Zhang, A nested grid mesoscale atmospheric chemistry model, *J. Geophys. Res.*, *96*, 3065–3084, 1991.
- Roelofs, G. J., and J. Lelieveld, Model study of the influence of cross-tropopause O₃ transports on tropospheric O₃ levels, *Tellus*, *49B*, 38–55, 1997.
- Russell, A., and R. Dennis, NASTRO critical review of photochemical models and modelling, *Atmos. Environ.*, *34*, 2283–2324, 2000.
- Sillman, S., J. A. Logan, and S. C. Wolfsy, The sensitivity of ozone to nitrogen oxides and hydrocarbons in regional ozone episodes, *J. Geophys. Res.*, *95*, 1837–1851, 1990.
- Simpson, D., et al., Inventorying emissions from nature in Europe, *J. Geophys. Res.*, *104*, 8113–8152, 1999.
- Singh, H. B., and D. J. Jacob, Future directions: Satellite observations of tropospheric chemistry, *Atmos. Environ.*, *34*, 4399–4401, 2000.
- Smolarkiewicz, P. K., A simple positive definite advection scheme with small implicit diffusion, *Mon. Weather Rev.*, *111*, 479–486, 1983.
- Smolarkiewicz, P. K., A fully multidimensional positive definite advection transport algorithm with small implicit diffusion, *J. Comp. Phys.*, *54*, 325–362, 1984.
- Stockwell, W. R., P. Middleton, J. S. Chang, and X. Tang, The second generation regional acid deposition model: Chemical mechanism for regional air quality modelling, *J. Geophys. Res.*, *95*, 16,343–16,367, 1990.
- Stohl, A., and T. Trickl, A textbook example of long-range transport: Simultaneous observation of ozone maxima of stratospheric and North American origin in the free troposphere over Europe, *J. Geophys. Res.*, *104*, 30,445–30,462, 1999.
- Tiedtke, M., A comprehensive mass flux scheme for cumulus parameterization in large-scale models, *Mon. Weather Rev.*, *117*, 1778–1800, 1989.
- Umweltbundesamt (German Environmental Agency), Luft kennt keine Grenzen, 6. Auflage, Berlin, Germany, 2001.
- Walcek, C. J., and G. R. Taylor, A theoretical method for computing vertical distributions of acidity and sulfate production within cumulus clouds, *J. Atmos. Sci.*, *43*, 339–355, 1986.
- Wang, Y., D. J. Jacob, and J. A. Logan, Global simulation of tropospheric O₃-NO_x-hydrocarbon chemistry, 1, Formulation, *J. Geophys. Res.*, *103*, 10,713–10,725, 1998.
- Waibel, A. E., H. Fischer, F. G. Wienhold, P. C. Siegmund, B. Lee, J. Stroem, J. Lelieveld, and P. J. Crutzen, Highly elevated carbon monoxide concentrations in the upper troposphere and lowermost stratosphere at northern midlatitudes during the STREAM II campaign in 1994, *Chemosphere: Global Change Science*, *1*, 233–248, 1999.
- Wesley, M. L., Parameterization of surface resistances to gaseous dry deposition in regional-scale numerical models, *Atmos. Environ.*, *23*, 1293–1304, 1989.

S. E. Bauer, Laboratoire des Sciences du Climat et de l'Environnement (LSCE), CEA-CNRS, CE SACLAY, L'Orme des Merisiers, F-91191 Gif-sur Yvette Cedex, France. (bauer@lsce.saclay.cea.fr)

I. Bey, Swiss Federal Institute of Technology (EPFL), EPFL-ENAC-LMCA, Batiment Chimie, CH-1015 Lausanne, Switzerland. (isabelle.bey@epfl.ch)

B. Langmann, Max-Planck-Institut für Meteorologie, Bundesstr. 55, D-20146 Hamburg, Germany. (langmann@dkrz.de)